

Commun. Theor. Phys. **75** (2023) 125504 (10pp) https://doi.org/10.1088/1572-9494/ad109c

Stable bulk nanobubbles can be regarded as gaseous analogues of microemulsions

Changsheng Chen, Hongguang Zhang and Xianren Zhang

State Key Laboratory of Organic–Inorganic Composites, Beijing University of Chemical Technology, Beijing 100029, China

E-mail: zhangxr@mail.buct.edu.cn

Received 18 September 2023, revised 29 November 2023
Accepted for publication 29 November 2023
Published 20 December 2023

Abstract

In our previous work [2022 *Phys. Chem. Chem. Phys*. **24** 9685], we used molecular dynamics simulations to show that bulk nanobubbles can be stabilized by forming a compressed amphiphile monolayer at bubble interfaces. This observation closely matches the origin of stability of microemulsions and inspired us to propose here that, in certain cases, stable bulk nanobubbles can be regarded as gaseous analogues of microemulsions: the nanobubble phase and the bubble-containing solution phase coexist with the external gas phase. This three-phase coexistence is then validated by molecular dynamics simulations. The stability mechanism for bulk nanobubbles is thus given: the formation of a compressed amphiphilic monolayer because of microbubble shrinking leads to a vanishing surface tension, and consequently the curvature energy of the monolayer dominates the thermodynamic stability of bulk nanobubbles. With the monolayer model, we further interpret several strange behaviors of bulk nanobubbles: gas supersaturation is not a prerequisite for nanobubble stability because of the vanishing surface tension, and the typical nanobubble size of 100 nm can be explained through the small bending constant of the monolayer. Finally, through analyzing the compressed amphiphile monolayer model we propose that bulk nanobubbles can exist ubiquitously in aqueous solutions.

Supplementary material for this article is available online

Keywords: bulk nanobubble, stability, compressed monolayer, three-phase equilibrium

1. Introduction

Bulk nanobubbles (BNBs) are spherical bubbles of sub-micrometer size, typically 100 nm, suspended in aqueous solution [1–4]. Their discovery originated in early studies on ultrasound and cavitation [5], and indirect evidence for the existence of bulk tiny bubbles was then given in a sonar study [6]. After 2000, experimental reports on nanobubbles emerged due to the extensive use of advanced experimental techniques, including dynamic light scattering, phase microscopy, infrared spectroscopy and nanoparticle tracking analyzers [7–10]. BNBs have aroused strong interest due to their long lifetime and numerous applications, such as water treatment [11–14], agriculture [15, 16], biomedicine [17, 18] and micro-reactors [19].

The unexpected stability of BNBs seems to contradict classical theory. According to the Epstein–Plesset theory [20], a bubble of radius 100 nm will have an internal pressure about 14.4 times atmospheric pressure and would dissolve within 1 μs. However, experiments reported that the period of existence of observed nanobubbles ranged from several hours to weeks [4, 7–10]. Such a long lifetime indicates that the reported BNBs are in fact thermodynamically stable.

Obviously, new theories are needed to explain BNB stability. The mechanisms proposed in the last 20 years for BNB stability can be divided into two categories: the enrichment of interfacial charges (zeta potential) [21, 22] and the adsorption of contaminants [23, 24]. Although these models are partly capable of explaining why BNBs are stable, there are some phenomena that cannot be explained by these models: the stability of BNBs at low gas saturation or at zeta potentials close to 0 [25–27] and their almost constant size (∼100 nm) in different reports [26–29].

In detail, for both mechanisms the stable radius of nanobubbles always depends on the number of charges and of contaminants enriched on the nanobubble interface. If the

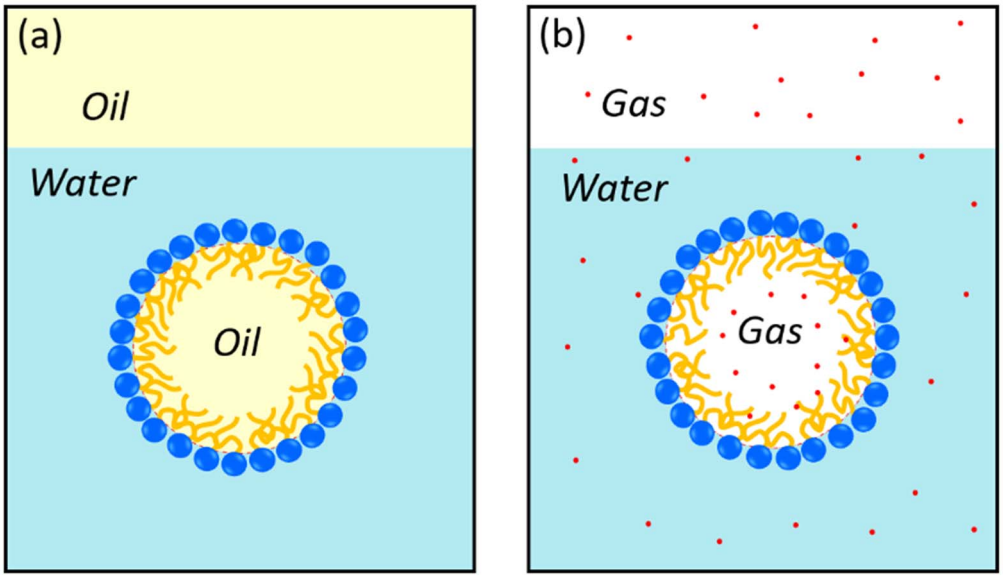

Figure 1. The similarities and differences between microemulsions and BNBs at small surfactant concentrations. (a) The oil-in-water microemulsion phase coexisting with an excess oil phase. (b) Nanobubble-containing aqueous solution that coexists with an excess gas phase. For the oil-in-water microemulsion, the oil droplet (colored in yellow) is encapsulated by a surfactant monolayer in a continuous phase of water, while for the BNB the gas bubble is encapsulated with a compressed amphiphile monolayer in the aqueous solution. In both cases, amphiphile molecules (or surfactants composed of a hydrophilic head in blue and a hydrophobic tail in orange) play an important role in their stability.

number of charges and adsorbed contaminants changes, stable nanobubbles of any size can be possible. However, the experimentally reported nanobubble size is often around 100 nm [26–29]. In addition, both the zeta potential and the contaminant mechanisms [23, 24] require the dissolved gas to reach a certain level of supersaturation, which provides an additional pressure (Laplace pressure) to balance the surface tension of bubble interfaces. This requirement is obvious in molecular dynamics (MD) simulations of BNB stability. Weijs *et al* [30] proposed with MD simulations that diffusive shielding stabilizes BNB clusters. Through MD simulations, Gao *et al* [31], Hewage and Meegoda [32] and Dixit and Das [33] further analyzed the performance of BNBs at certain levels of gas supersaturation. These studies help us to understand the properties of BNBs. However, the results of these studies still partly contrast with some experimental observations that BNBs remain stable for a long time at rather low gas saturations ($S \sim 0$) [25] as a result of the exposure of nanobubble solutions to the ambient atmosphere. Experiments also show that, at least for certain cases [26] at low gas saturation, the required interfacial charge density and zeta potential for stabilizing BNBs [22] are out of reach. These disagreements demonstrate the existence of some important unidentified characteristics for the stabilization mechanism of real nanobubbles: the stabilization mechanism of BNBs is still an open question.

In our recent work [34], we found that adsorption of amphiphiles (organic contaminants or surfactants) with certain structures can lead to stable nanobubbles. With the dissolution of gas in a large bubble, the areal density of amphiphiles at the bubble interface becomes increasingly high, and correspondingly the surface tension decreases. Once a compressed amphiphilic monolayer is formed, the BNB becomes stable with a vanishing surface tension [34]. These findings demonstrate an obvious similarity between BNBs and microemulsions. Microemulsions are known to be thermodynamically stable, with a well-interpreted stability mechanism [35–38].

This similarity inspires us to explore the theory of BNB stability, in analogy with microemulsions. By extending our simulation results [34], in this work we further propose that BNBs can be regarded as gaseous analogues of microemulsions: in nanobubble systems the bubble phase and the solution phase coexist with the external gas phase (see figure 1). We analyze the characteristics of stable BNBs from the following aspects: (i) the similarity between nanobubbles and microemulsions; (ii) shrinking of large bubbles and the adsorption of amphiphilic molecules causing the formation of a compressed amphiphilic monolayer at nanobubble interfaces; (iii) thermodynamic analysis of three-phase coexistence of BNB systems, which is then validated with molecular simulation; (iv) determination of nanobubble size from the rigidity of the compressed amphiphilic monolayer; (v) trace organic contaminants as a source of amphiphiles for the formation of a compressed amphiphilic monolayer.

2. Results and discussion

2.1. The similarity between BNBs and microemulsions

Microemulsions are thermodynamically stable, isotropic liquid mixtures of two immiscible fluids, stabilized by amphiphilic surfactants [35–41]. According to the IUPAC definition, a microemulsion is a ‘dispersion made of water,

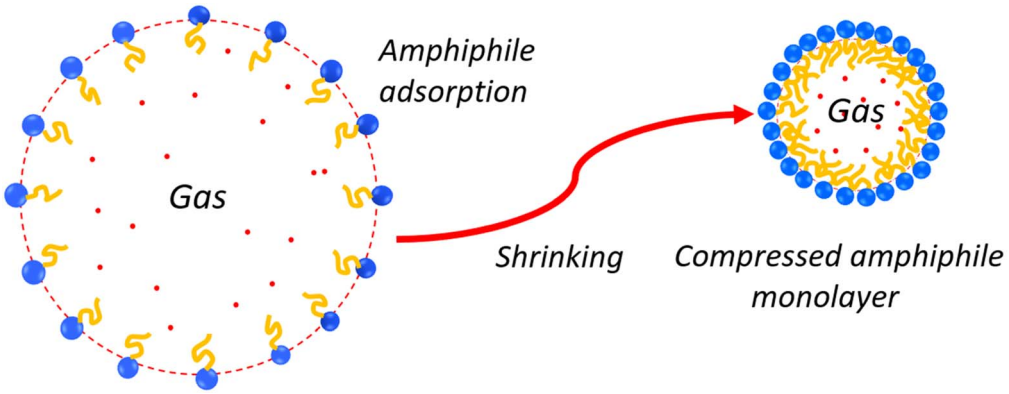

Figure 2. Schematic drawing of the formation of a compressed amphiphilic monolayer when a microbubble shrinks. The shrinking of a large bubble leads to a decrease in surface tension. Once a minimum in the average area occupied by each surfactant molecule is reached, a compressed amphiphile monolayer is formed. For the compressed amphiphile monolayer, the interfacial free energy for the nanobubble is dominated by the curvature free energy.

oil, and surfactant(s) that is an isotropic and thermodynamically stable system' [41, 42]. The typical size of oil-in-water (O/W) microemulsions is close to the experimentally observed diameter of long-lived BNBs (∼100 nm). As schematically shown in figure 1(a), an O/W microemulsion mainly contains three components: solvent (water), surfactant molecules forming the monolayer and oil molecules encapsulated by the monolayer and/or in the excess phase. The whole system is in a coexistence state (Winsor I domain in the Winsor classification) [43]: the O/W microemulsion phase coexisting with an excess oil phase. Such a system exhibits an ultralow interfacial tension, and so far the thermodynamic stability and polymorphic coexistence of microemulsions have been well explained [37–40].

The similarity between BNBs and microemulsions can be summarized as follows. (i) They are both nanoscale entities observed in experiments, with a typical size of ∼100 nm. (ii) Both are thermodynamically stable, although the underlying stabilization mechanism for BNBs [29–32] is still under debate. (iii) Surfactant monolayers on their interfaces play an essential role in their stability. Careful experiments [24] have proved that trace organic contaminants are necessary for nanobubble stabilization, and we further demonstrated that a compressed amphiphile monolayer is required for nanobubble stability at low gas supersaturation [34]. (iv) The vanishing interfacial tension would provide a necessary condition for stability, both for microemulsions and for BNBs. For stable BNBs at low gas supersaturation, the vanishing surface tension comes from the dissolution of gas bubbles, which decreases the bubble area until an ultralow surface tension is reached [34]. This is again similar to microemulsions. A microemulsion is recognized as a thermodynamically stable object, and the extremely low interfacial tension is the key to its stability.

Based on the aforementioned similarities between BNBs and microemulsions, we further propose that stable BNBs are a special kind of microemulsion, with the oil in the O/W microemulsion simply being replaced with insoluble or slightly soluble gas (see figure 1(b)). Here we will first give the stability mechanism for BNBs; then we will use the mechanism to interpret some strange behaviors of BNBs reported experimentally.

We also need to point out the difference between BNBs and microemulsions: in BNBs the tail groups of surfactants in the monolayer contact gas molecules, while for microemulsions it is oil molecules (figure 1). This difference may lead to different requirements for obtaining ultralow interfacial tension. Regarding the analysis of microemulsion stability, Winsor [44] proposed the so-called R ratio, $R_{ratio} = \frac{A_{CO}}{A_{CW}}$, where A_{CO} represents the molecular interactions (per unit interface area) between the tail groups of the surfactant and oil molecules and A_{CW} those between surfactant heads and water molecules. For microemulsions, ultralow interfacial tension ($R_{ratio} = 1$) can be achieved by changing either A_{CO} or A_{CW}. For BNBs with water–gas interfaces, R_{ratio} should be rewritten as $R_{ratio} = \frac{A_{CG}}{A_{CW}}$. Here A_{CG}, which comes mainly from tail–tail interactions since the tail–gas interaction is rather weak, is difficult to change. However, ultralow interfacial tension can still be achieved by modulating A_{CG} through altering the ionic or steric repulsion between neighboring head groups by various means, such as adding saline solution or co-surfactant.

2.2. The compressed amphiphilic monolayer model and the stabilization mechanism of BNBs

The similarity of BNBs and microemulsions leads us to propose a compressed amphiphilic monolayer model for BNB stability. In this mechanism, we assume that most stable BNBs come from the shrinking of large bubbles, for example microbubbles, as suggested in numerous studies [22–24, 45, 46]. Experimentally, microbubbles can be generated by shaking [47], ultrasound [26, 28] and alcohol–water exchange [29]. Alternatively, swelling of micelles at high gas supersaturation or macrobubble collapse can also induce microbubbles. Then, at low gas supersaturation the gas dissolution causes the shrinkage of the microbubbles until a compressed amphiphilic monolayer is formed at the bubble interface, which would lead to the formation of stable BNBs (see figure 2).

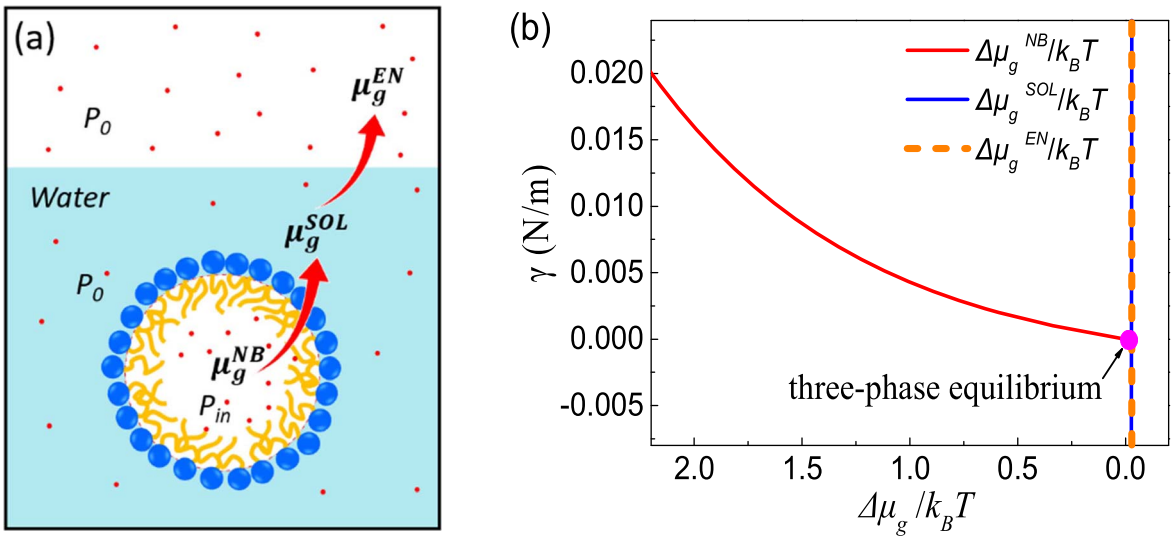

Figure 3. Schematic of three-phase equilibrium. (a) The chemical equilibrium of gas at different phases. μ_g^{NB}, μ_g^{SOL} and μ_g^{EN} are the chemical potentials of the gas inside the bubble, in solution and in the environment, respectively. The chemical equilibrium for gas molecules requires $\mu_g^{NB} = \mu_g^{SOL} = \mu_g^{EN}$. (b) The required gas–liquid surface tension for a BNB in mechanical equilibrium with its surrounding as a function of the chemical potential for gas inside the nanobubble, under the conditions of $P_0 \approx 100$ kPa and $R \approx 50$ nm. For the purpose of simplification in the figure we assume that the gas in solution and the gas in the environment are in chemical equilibrium, namely, $\mu_g^{SOL} = \mu_g^{EN}$. The pink dot indicates the particular situation where the chemical potentials for the three phases are the same, i.e. three-phase coexistence.

During the process of microbubble shrinking, the gradual adsorption of amphiphilic molecules and decrease in bubble area would lead to the interfacial enrichment of amphiphiles for both insoluble and soluble surfactants. For soluble surfactants the enrichment may be because the typical time of surfactant desorption is larger than that for bubble shrinking. The increasing areal density of surfactant at the interface would lead to a decrease in surface tension until a certain value of areal density is reached (see figure 2). Once an extremely low (close to 0) surface tension is reached [34], the compressed amphiphilic monolayer is regarded as being formed. When the monolayer is further compressed, the decreasing average area occupied by each surfactant would become highly energetically unfavorable. Instead, the monolayer can deform in the normal direction (bending) and therefore the interfacial free energy per nanobubble is dominated by the curvature free energy.

2.3. The mechanical and chemical equilibriums of BNBs in three-phase coexistence

In particular cases, the remarkable long lifetime of BNBs is related to the thermodynamic equilibria of different phases: the dispersed BNB phase, the solution saturated with dissolved gas and the ambient gas phase. Therefore, the whole system containing stable BNBs is a three-phase coexistence state. Here we analyze how gas equilibrates in the three phases from the corresponding driving force, i.e. the chemical potential of the gas. We will show that within the framework of the compressed amphiphile monolayer model, both the mechanical and chemical equilibrium of BNBs could be reached, even in a gas-saturated solution. For stable BNBs in such a gas-saturated state we will deduce the vanishing interfacial tension from the quality of three chemical potentials, namely the equality of chemical potentials is the cause and the vanishing surface tension is the result.

The requirement for chemical equilibrium of gas molecules is schematically shown in figure 3(a). Since the partial pressure for solvent is negligibly small inside the nanobubble, only dissolved gas was taken into account here [2, 3, 20–23]. Gas in the nanobubble can be simplified as ideal gas, and the corresponding chemical potential μ_g^{NB} is

$$\mu_g^{NB} = \mu_g^{sat} + k_B T \bullet \ln\frac{P_{in}}{P_{sat}}. \tag{1}$$

For gas dissolved in solution the chemical potential, μ_g^{SOL}, is given by

$$\mu_g^{SOL} = \mu_g^{sat} + k_B T \bullet \ln\left(\frac{c_g}{c_g^{sat}}\right) \tag{2}$$

where μ_g^{EN} is the chemical potential of gas in the external gas phase and

$$\mu_g^{EN} = \mu_g^{sat} + k_B T \bullet \ln\frac{P_0}{P_{sat}}. \tag{3}$$

In above equations, P_0 is the ambient pressure, P_{in} is the pressure of gas inside the bubble and c_g is the actual gas solubility that equilibrates with the bubble. Here a reference state at a pressure P_{sat} is chosen with the gas is saturated in solution, and μ_g^{sat} and c_g^{sat} are the corresponding chemical potential and solubility of the dissolved gas.

Therefore, for a nanobubble in a state of thermodynamic equilibrium, the equality of chemical potential for gas molecules requires

$$\mu_g^{NB} = \mu_g^{SOL} = \mu_g^{EN}. \tag{4}$$

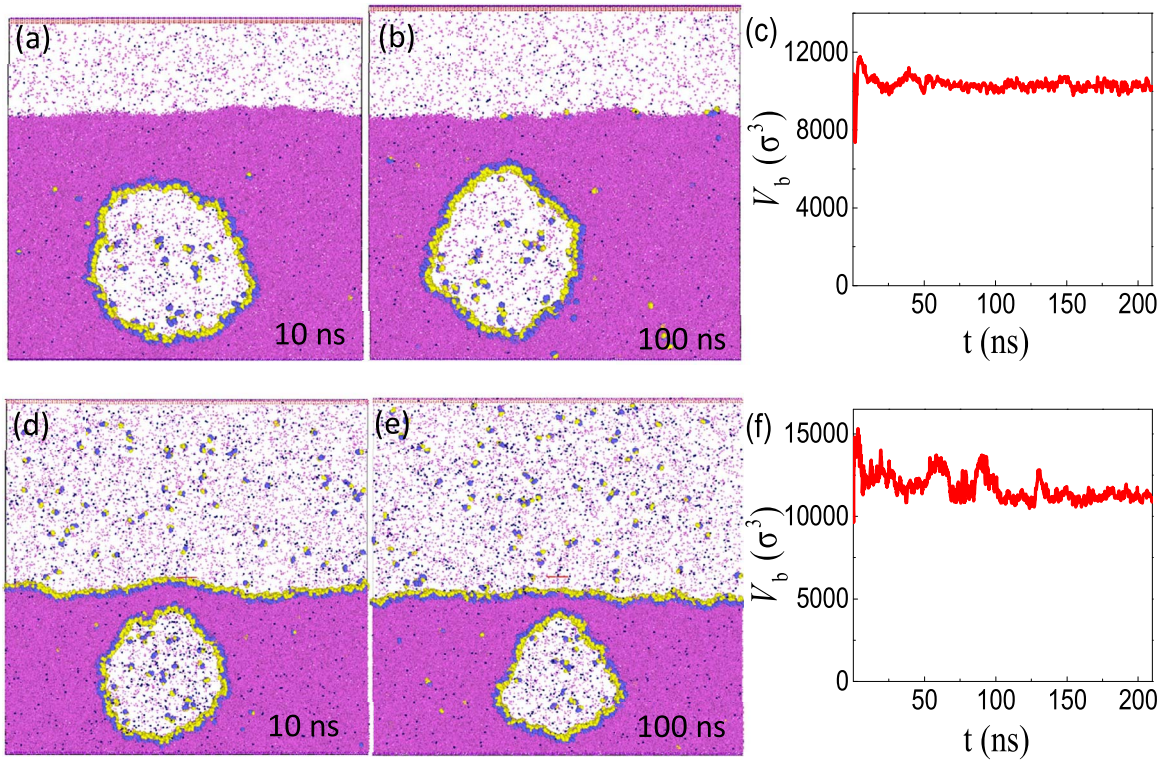

Figure 4. Verifying the three-phase equilibrium with MD simulation. (a), (b) Two typical snapshots for a BNB fully covered by H_5T_3 surfactant molecules. (c) The time evolution of the bubble size. In this case, the numbers of surfactant, liquid and gas molecules added are 492, 121 848 and 768, respectively. (d)–(f) A different situation in which both the bubble and the flat gas–liquid interface are covered by H_5T_3 surfactant molecules. In this case the numbers of surfactant, liquid and gas molecules added are 1092, 162 936, and 1952, respectively.

Figure 3(b) shows that the chemical potential of gas confined in the bubble μ_g^{NB} gradually approaches μ_g^{SOL} and μ_g^{EN} with the decrease of interfacial area during the process of monolayer compression. Equation (1) leads to $\mu_g^{NB} - \mu_g^{SOL} = k_B T \bullet \ln\left(\frac{P_{in} c_g^{sat}}{P_{sat} c_g}\right) = 0$ and $\mu_g^{NB} - \mu_g^{EN} = k_B\ T \bullet \ln\frac{P_{in}}{P_0} = 0$, which give rise to

$$P_{in} = P_0 \quad \text{and} \quad \frac{P_{in} c_g^{sat}}{P_{sat} c_g} = 1. \tag{5}$$

The mechanical equilibrium can be described by the Laplace equation $\Delta P = \frac{2\gamma}{R}$. The Laplace equation, along with $P_{in} = P_0$, gives rise to an ultralow surface tension ($\gamma \approx 0$) for stable nanobubbles. Therefore, the vanishing surface tension is a consequence of the thermodynamic (both mechanical and chemical) requirement for stable BNBs.

Then we analyze what $\frac{P_{in} c_g^{sat}}{P_{sat} c_g} = 1$ means. We define S as the supersaturation of the gas at ambient pressure P_0, and $S = c_g/c_g^0 - 1$, with c_g^0 the saturated solubility at ambient pressure P_0. According to Henry's law, $c_g = HP_{in}$ and $c_g^0 = HP_0$, with H the coefficient of Henry's law. Thus, we have $SP_0 = P_{in} - P_0 \approx 0$, which means $S \approx 0$. This is also consistent with the experimental observations that even at low gas supersaturation ($S \approx 0$) a large number of BNBs can exist stably [25].

Note that until now we have not considered the effect of bending energy of the surfactant monolayer. We will demonstrate in a subsequent section that by taking into account the monolayer rigidity, a small but not exactly zero surface tension is sufficient to stabilize BNBs.

2.4. MD simulations validate that three-phase equilibrium can be reached

The three-phase equilibrium coexistence mechanism for a nanobubble system (figure 3(a)) can be verified through MD simulations. Unlike our previous MD simulations for two-phase (nanobubble phase and solution phase) coexistence [34], here we considered three-phase equilibrium: a BNB dispersed in a solution coexisting with an ambient gas phase (figure 4). A number of surfactant molecules, H_5T_3, which are nearly insoluble in solvent, were initially distributed near either the bubble interface or the gas–liquid interface. A given number of gas molecules were inserted into the pre-existing bubble and/or into the gas phase above the solution. The isotropic isobaric ensemble (NPT) was performed at temperature $T = 0.846\varepsilon/k_B$ and pressure $P = 0.0122\varepsilon\sigma^{-3}$. The simulation methods and detailed parameters are summarized in the Supplementary Information, and more details can be obtained from our previous work [34]. Note that the effect of charge enrichment is not taken into account in our simulations.

The extensive simulation runs demonstrate that the surfactant would rapidly reach the bubble interface and form a surfactant monolayer. In several cases with a sufficient number of surfactant molecules adsorbed on the bubble

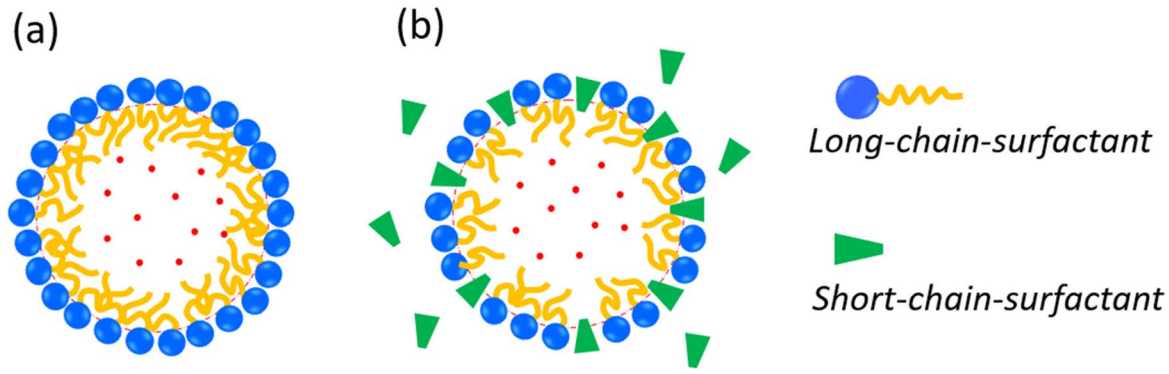

Figure 5. Schematic drawing of two different models for the compressed amphiphile monolayer: (a) the monolayer comprises only long-chain-surfactant molecules and (b) the monolayer contains both long-chain and short-chain surfactant molecules.

interface the nanobubble may become stable, although dramatic exchange of gas molecules in three phases and strong shape fluctuation of the bubble are observed.

The typical simulation results are shown in figures 4(a)–(c). Figure 4(c) gives the evolution of the bubble volume over time. The figure indicates that although the bubble volume changes sharply in the initial stage of simulation, the bubble size then fluctuates around a constant size, demonstrating that the nanobubble has reached both mechanical and chemical equilibrium with its surroundings. We also simulated different cases with various numbers of surfactant molecules. The simulation results (see, e.g., figures 4(d)–(f)) show that adding more surfactant would lead to extra adsorption of surfactant at the flat gas–liquid interface, while the BNB remains stable. In general, both cases in figure 4 validate the three-phase coexistence mechanism for stable BNBs displayed in figure 3(a).

For the stable nanobubbles obtained, we also extended the simulation time to 300 ns. As expected, coexistence of the three phases continued (see figures S2(a)–(b) in the SI). The figures clearly show that the nanobubbles are still stable.

2.5. Nanobubble size can be estimated from the rigidity of the compressed amphiphile monolayers

We now turn to the question of why the typical size of BNBs observed experimentally is around 100 nm. First, we stress again that once a compressed amphiphilic monolayer is formed it shows a tendency to resist certain changes in its curvature. This is because, for the compressed monolayer, further decrease in the monolayer area would become energetically unfavorable. In contrast, a compressed monolayer can deform more easily in the bending mode and thus the interfacial deformation of the nanobubble is dominated by the curvature free energy. This curvature energy for a tensionless monolayer with a curvature that deviates from its spontaneous curvature was emphasized by Helfrich [48]. Accordingly, the interfacial free energy of the surfactant monolayer reads

$$F_{\mathrm{s}} = \int \left[f_0 + \frac{\kappa}{2}(c_1 + c_2 - 2c_0)^2 + \bar{\kappa} c_1 c_2 \right] \mathrm{d}A, \qquad (6)$$

in which κ is the bending rigidity, $\bar{\kappa}$ is the saddle-splay modulus and f_0 is the interfacial tension of the surfactant monolayer without considering bending energy [49]. The spontaneous curvature, $c_0 = 1/R_0$, with R_0 the spontaneous radius of curvature, reflects the asymmetry between the inside and outside of the monolayer. For a spherical nanobubble, the actual curvature $c_1 = c_2 = 1/R$, and thus $F_{\mathrm{s}} = \int [\gamma_0 - \frac{4\kappa}{R_0}\left(\frac{1}{R}\right) + (2\kappa + \bar{\kappa})\left(\frac{1}{R}\right)^2] \mathrm{d}A$. Here, $\gamma_0 = f_0 + 2c_0^2$ is the interfacial energy of the planar surfactant monolayer per unit area [49]. When the surfactant monolayer is flat, the actual curvature $c_1 = c_2 = 0$ and the interfacial free energy of the surfactant monolayer $F_{\mathrm{s}} = \int \gamma_0 \mathrm{d}A$.

The spontaneous curvature c_0 and the bending stiffness κ of surfactant monolayers are important factors that determine nanobubble size. κ can decrease strongly once mixtures of surfactants of different chain lengths are introduced because of the resulting disorder of surfactant chains [50]. Szleifer *et al* [50] found that for a one-component surfactant membrane κ increases from $k_{\mathrm{B}}T$ to tens of $k_{\mathrm{B}}T$ by increasing the chain length or decreasing the area per surfactant molecule. They also demonstrated that addition of relatively short-chain alcohol or other co-surfactant additives is sufficient to lower the bending constant by an order of magnitude. Based on these findings [50], we suppose that there exist different situations for a compressed amphiphilic monolayer of BNBs depending on the experimental conditions (see figure 5).

For the first case (figure 5(a)), for which a single type of large and insoluble surfactant comprises the monolayer, the stiffness κ of the compressed monolayer for BNBs is rather large ($\kappa >> 1k_{\mathrm{B}}T$) [38, 51]. With equation (6), the minimization of F_s with respective to bubble radius at constant total area A (or equivalently, the fixed number of surfactant molecules at the nanobubble interface) gives the optimal bubble radius R_{e} with [38, 51, 52]

$$\frac{R_{\mathrm{e}}}{R_0} = \frac{2\kappa + \bar{\kappa}}{2\kappa}. \qquad (7)$$

Therefore, for a stiff monolayer ($\kappa > 10\ k_{\mathrm{B}}T$), the minimized bending free energy F_s will force the equilibrium size of the nanobubble to approach R_0 because $\bar{\kappa}$ is relatively small [39, 40]. In other words, it is the spontaneous curvature $c_0 = 1/R_0$ that determines the size of BNBs. c_0 or R_0 can be directly related to the packing parameter of amphiphilic molecules, indicating the tendency of the interface to curve toward either the water ($c_0 > 0$) or the gas ($c_0 < 0$). As shown

in our MD simulations [34], $c_0 < 0$ is required for stable nanobubbles.

The second situation is for a multicomponent amphiphilic monolayer (figure 5(b)), in which the mixing of long-chain and short-chain surfactants (e.g. alcohol) substantially lowers the bending constant κ [50]. We believe that this situation represents BNBs stabilized by trace organic contaminants. When κ is small enough (k_BT), it is the stiffness of monolayer κ rather than spontaneous curvature that dominates the observable bubble size. In this case, the competition between thermal and bending energies can be described by the notion of persistence length ξ_k, which plays an essential role in determining nanobubble size, as for microemulsions [38–40, 53].

Following Helfrich [53]and Peliti and Leibler [49], we assume that a stable nanobubble would reach its actual size $R \approx \xi_k$ when the effective stiffness κ_e approaches zero. The effective stiffness is determined by [49]

$$\kappa_e = \kappa + \frac{3k_BT}{4\pi}\ln(q\xi_0), \tag{8}$$

with ξ_0 the molecular length close to the surfactant layer thickness and wave number q (with $\xi_k \sim q^{-1}$) in the thermal fluctuation process. For nanobubbles with a soft monolayer, equation (8) leads to

$$\xi_k = \xi_0 \exp\left(\frac{4\pi\kappa}{3k_BT}\right). \tag{9}$$

Note that a similar equation was given for microemulsions [53], with $4\pi/3$ replaced by 2π [38, 51]. Here we determine bubble ξ_k for BNBs by setting the typical stiffness of flexible surfactant monolayers around $1k_BT$ [50], i.e. $\kappa \sim k_BT$. When we choose the typical values for a surfactant monolayer, $\xi_0 \sim 10$Å [38–40] and $\kappa \sim 1k_B$T [50], equation (9) gives $\xi_k \approx 65.8$ nm. Thus, the bubble size predicted from the compressed amphiphilic monolayer model is roughly consistent with the experimentally observed values that are mostly around 100 nm (diameter) [24, 25].

For flexible amphiphilic monolayers, the typical stiffness κ reported experimentally is close to $1k_BT$, i.e. 0.8–1.2 k_BT [38–40, 50–52]. With equation (9), we can therefore predict the size of a stable BNB (figure 6). The range of predicted bubble radii is consistent with those from experimental observations (about 40–150 nm) [24–29].

If the stiffness κ of the monolayer is further reduced, κ is much smaller than k_BT. ξ_k is of the order of a molecule's length. In this case, well-defined surfactant monolayers become unstable due to the dominant shape and thermal fluctuation. Thus, the nanobubble structure becomes unstable and one would obtain a micelle-like structure [34].

In general, we distinguish two different situations, both leading to compressed amphiphilic monolayers that can stabilize BNBs. The first corresponds to a one-component rigid monolayer. In this case, the bulk size is mainly controlled by the spontaneous radius of curvature, R_0, which is directly related to the packing parameter of amphiphilic molecules. The second situation corresponds to a multicomponent soft monolayer, which is featured with a lower bending constant,

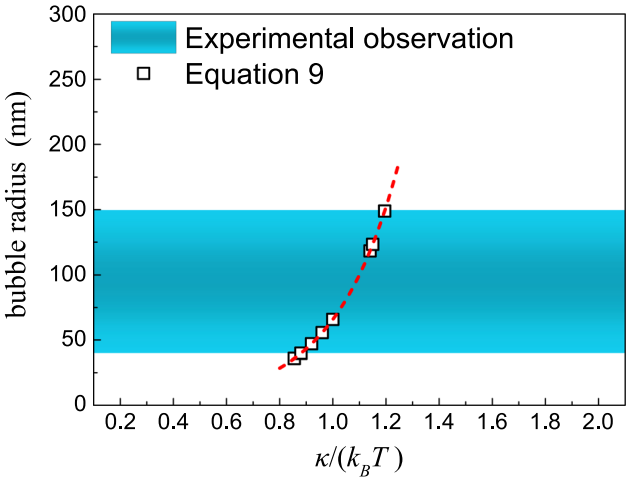

Figure 6. Comparison of predicted nanobubble radius (equation (9)) with the range of radii of stable nanobubbles reported experimentally. The symbols indicate the predicted bubble sizes with the stiffness κ given in literature [37–39, 48–51]. The shaded areas indicate the size range of stable BNBs observed experimentally.

$\kappa \sim k_B$T. In this case the bubble size would be around 100 nm. In case of $\kappa << k_BT$ the nanobubbles would become unstable and micelle-like structures are preferred.

2.6. The ubiquitous existence of BNBs in aqueous solutions

Here we focus on an open question for the compressed amphiphile monolayer model: where do the amphiphilic molecules come from? First, we will illustrate that even trace organic contaminants in solution can provide amphiphilic molecules to stabilize BNBs. Then we propose that BNBs can exist ubiquitously in aqueous solutions.

A careful experimental work [24] shows that concentration of the generated BNBs becomes negligible if various source of contaminants are properly avoided. This clearly indicates that trace organic contaminants are necessary for nanobubble stabilization. However, at present it is still difficult to avoid contaminants completely: they may come from the gas source, from exposure of the solution surface to airborne contaminants, from the contacting solid or from the solution itself.

Here we just illustrate that even a small quantity of trace organic contaminants dissolved in a so-called 'pure' solvent is sufficient to supply the amphiphile molecules for stabilizing a large number of BNBs. To analyze whether this small level of contaminants is sufficient to stabilize the BNBs we take the radius of the nanobubble as $R = 50$ nm and assume that the cross-sectional area a of the surfactant molecule is about 9 Å^2 which is close to the values reported in the literature [54–58]. For a single nanobubble of 100 nm, the number of surfactant molecules n_1 required for the compressed monolayer can be estimated as $n_1 = \frac{4\pi R^2}{a} \approx 3.49\times10^5$. The total number of surfactant molecules needed for all BNBs in 1 ml of solution is about $N_1 = n_1 c_{NB} \approx 3.49\times10^{13}$. Here the typical concentration of BNBs, $c_{NB} \sim 10^8$ ml^{-1}, was used [26–29].

Then we roughly estimated the amount of surfactant existing in the solution from the reported carbon content

(TC), which mainly comes from organic contaminants in the solution and acts as a surfactant. In nanobubble experiments the TC of pure water is often given, with a typical value of <50 parts per billion (ppb). Here we can approximate the concentration of surfactants (contaminants) in water, $c_{\rm surf}$, by a typical TC value of 24 ppb [59]. The total number of surfactant molecules N_2 actually contained in 1 ml of water can be estimated by $N_2 = \frac{1\,{\rm g}\times c_{\rm surf}}{M_{\rm surf}} \times N_{\rm A} \approx 5 \times 10^{13}$. Here $M_{\rm surf}$ is the molar mass of the surfactant, having a value of 288 g mol^{-1} with reference to sodium dodecyl sulfate, and N_A is the Avogadro's constant. If we assume that 60% of the TC consists of surfactants, $N_2^{\cdot} = N_2 \times 60\% \approx 3 \times 10^{13}$. It is clear that $N_2^{\cdot} = N_{\rm l}$, meaning that even the ultrapure water used in experiments still contains a sufficient quantity of contaminants to stabilize BNBs with a typical nanobubble concentration of $c_{\rm NB} \approx 10^8$ ml^{-1}.

Note that this is just a rough estimate, without considering the distribution of the organic contaminants between dissolution and the nanobubble interface. If the distribution is taken into account, the concentration of stable BNBs would decrease. This agrees with the experimental observations that nanobubble concentration would substantially reduce if the solution was carefully prepared to remove different sources of organic contaminants [24]. However, the trace organic contaminants dissolved in the solution itself are not the only source of amphiphilic molecules. They may also come from, for example, exposure of the solution surface to airborne contaminants and the container. Several reports have demonstrated that graphite surfaces exposed to air may accumulate a thin organic layer [60–62]. Regardless of where they come from, organic contaminants and other factors have been used to interpret the stability and behavior of interfacial nanobubbles [63–66].

When there is surfactant adsorption, the compressed amphiphilic monolayer model allows us to anticipate the ubiquitous presence of BNBs in some aqueous solution, with a greater or lesser bubble concentration. This ubiquity is based on the following facts: the unavoidable presence of trace organic contaminants may act as a source of amphiphiles; adsorption of amphiphiles and shrinking of large bubbles leads to the formation of a compressed amphiphile monolayer; and BNBs with such a compressed monolayer are thermodynamically stable in some cases. Therefore, we can conclude that the appearance of BNBs may be much more common than we expected, in particular in an aqueous solution exposed to the ambient atmosphere.

3. Conclusion

The stabilization mechanism of BNBs is still an open question. Based on our discovery of the existence of a compressed amphiphilic monolayer on stable nanobubbles [34], in this work we further proposed that BNBs can be regarded as gaseous analogues of microemulsions: the nanobubble phase and the bubble-containing solution phase coexist with the external gas phase. This three-phase coexistence was subsequently validated by MD simulations. The stability mechanism for BNBs is given as follows. The shrinking of large bubbles and adsorption of amphiphiles lead to the formation of a compressed amphiphilic monolayer at nanobubble interfaces. The compressed monolayer has an ultralow surface tension, and thus it is the curvature free energy, rather than surface tension, that dominates the interface free energy and nanobubble stability.

In the presence of surfactant adsorption, with the compressed amphiphilic monolayer model, we can interpret two mysterious experimental observations: the stability of BNBs at low gas saturation and stable nanobubbles often having a typical size of around ∼100 nm. For the first observation, the unexpected stability of BNBs at rather low gas saturations can be well interpreted by the ultralow surface tension of nanobubbles. Due to the formation of a tensionless amphiphilic monolayer, gas supersaturation is no longer a necessary condition for stability of BNBs. We also explained why the typical reported size of stable BNBs is often around 100 nm. We proposed that most experimentally reported BNBs are stabilized by adsorbed trace organic contaminants, the multicomponent nature of which leads to a very low bending constant κ of the formed monolayer. Under conditions of $\kappa \sim k_{\rm B}T$, a simple estimate from persistence length predicts a stable nanobubble size of around 100 nm.

We also suggest that BNBs can exist ubiquitously. We show that even the small amount of trace organic contaminants dissolved in chemically 'pure' solvent is sufficient to supply the amphiphilic molecules needed for stabilizing BNBs at a typical nanobubble concentration $c_{\rm NB} \sim 10^8$ ml^{-1}. In real situations, there are many more sources of organic contaminants that can stabilize BNBs. Therefore, the ubiquity of BNBs is a direct consequence of the compressed amphiphilic monolayer model: unavoidable existence of trace organic contaminants that act as a source of amphiphiles, and the interface adsorption of amphiphiles; shrinking of large bubbles that lead to the formation of a compressed amphiphilic monolayer; and the BNBs with such a monolayer being thermodynamically stable. The ubiquity of BNBs in some aqueous solutions may have significant effects on a variety of processes that are related to bubble formation and disappearance.

The stability mechanism presented here might offer guidelines for studying stable BNBs experimentally. (i) We can take inspiration from the extensive experimental study of microemulsions because of the similarity of stability mechanisms between nanobubbles and microemulsions. (ii) Pre-existing large bubbles (either microbubbles or macrobubbles) are essential for the generation of stable nanobubbles because nanobubbles come from the shrinking of large bubbles—spontaneous nucleation of nanobubbles seems unlikely at low levels of gas supersaturation. (iii) The simultaneous addition of both surfactant and co-surfactant may be more effectively in stabilizing nanobubbles. (iv) The elimination of nanobubbles requires control of the introduction of trace contaminants not only from water but also the ambient environment, and the instrumentation and electrophoretic removal of pre-existing charged nanobubbles if necessary.

Our findings offer a theoretical foundation for the stability of BNBs, but reliable experimental validation is needed to establish their existence. Additionally, it is important to note that the proposed model and the zeta potential model are not necessarily incompatible. Although we do not include the impact of enriched charges on the BNB interface in our model, this does not mean that the zeta potential does not play an important role in nanobubble stability. In fact, we think the two mechanisms should work in concert with one another, at least in some circumstances.

Acknowledgments

The work was supported by the National Natural Science Foundation of China (Grant Nos. 21978007 and 22278013).

ORCID iDs

Xianren Zhang https://orcid.org/0000-0002-8026-9012

References

[1] Alheshibri M *et al* 2016 A history of nanobubbles *Langmuir* **32** 11086–100
[2] Zhou L *et al* 2021 Generation and stability of bulk nanobubbles: a review and perspective *Curr. Opin. Colloid Interface Sci.* **53** 101439
[3] Tan B H, An H and Ohl C D 2021 Stability of surface and bulk nanobubbles *Curr. Opin. Colloid Interface Sci.* **53** 101428
[4] Nirmalkar N *et al* 2018 On the existence and stability of bulk nanobubbles *Langmuir* **34** 10964
[5] Sette D and Wanderlingh F 1962 Nucleation by cosmic rays in ultrasonic cavitation *Phys. Rev.* **125** 409
[6] Johnson B D and Cooke R C 1981 Generation of stabilized microbubbles in seawater *Science* **213** 209
[7] Ushikubo F Y *et al* 2010 Evidence of the existence and the stability of nano-bubbles in water *Colloids Surf.* A **361** 31
[8] Yasui K, Toru T and Wataru K 2018 Mysteries of bulk nanobubbles (ultrafine bubbles); stability and radical formation *Ultrason. Sonochem.* **48** 259
[9] Jin F *et al* 2007 Slow relaxation mode in mixtures of water and organic molecules: supramolecular structures or nanobubbles? *J. Phys. Chem. B* **111** 2255
[10] Sedlák M and Rak D 2014 On the origin of mesoscale structures in aqueous solutions of tertiary butyl alcohol: the mystery resolved *J. Phys. Chem. B* **118** 2726
[11] Atkinson A J *et al* 2019 Nanobubble technologies offer opportunities to improve water treatment *Acc. Chem. Res.* **52** 1196
[12] Agarwal A, Ng W J and Liu Y 2011 Principle and applications of microbubble and nanobubble technology for water treatment *Chemosphere* **84** 1175
[13] Li H *et al* 2014 Characteristics of micro-nano bubbles and potential application in groundwater bioremediation *Water Environ. Res.* **86** 844
[14] Haris S *et al* 2020 The use of micro-nano bubbles in groundwater remediation: a comprehensive review *Groundw. Sustain. Dev.* **11** 100463
[15] Sang H *et al* 2018 Effects of micro-nano bubble aerated irrigation and nitrogen fertilizer level on tillering, nitrogen uptake and utilization of early rice *Plant Soil. Environ.* **64** 297
[16] Schenk H J, Steppe K and Jansen S 2015 Nanobubbles: a new paradigm for air-seeding in xylem *Trends Plant Sci.* **20** 199
[17] Gao Z *et al* 2008 Drug-loaded nano/microbubbles for combining ultrasonography and targeted chemotherapy *Ultrasonics* **48** 260
[18] Oeffinger B and Wheatley M 2004 Development and characterization of a nano-scale contrast agent *Ultrasonics* **42** 343
[19] Paknahad A *et al* 2021 Biomedical nanobubbles and opportunities for microfluidics *RSC Adv.* **11** 32750
[20] Epstein P S and Plesset M S 1950 On the stability of gas bubbles in liquid-gas solutions *J. Chem. Phys.* **18** 1505
[21] Zhang H, Guo Z and Zhang X 2020 Surface enrichment of ions leads to the stability of bulk nanobubbles *Soft Matter* **16** 5470
[22] Tan B H, An H and Ohl C D 2020 How bulk nanobubbles might survive *Phys. Rev. Lett.* **124** 134503
[23] Wang S *et al* 2021 Collective dynamics of bulk nanobubbles with size-dependent surface tension *Langmuir* **37** 7986
[24] Eklund F and Swenson J 2018 Stable air nanobubbles in water: the importance of organic contaminants *Langmuir* **34** 11003
[25] Fang Z *et al* 2018 Formation and stability of surface/bulk nanobubbles produced by decompression at lower gas concentration *J. Phys. Chem. C* **122** 22418
[26] Nirmalkar N, Pacek A W and Barigou M 2019 Bulk nanobubbles from acoustically cavitated aqueous organic solvent mixtures *Langmuir* **35** 2188
[27] Jadhav A J and Barigou M 2020 Proving and interpreting the spontaneous formation of bulk nanobubbles in aqueous organic solvent solutions: effects of solvent type and content *Soft Matter* **16** 4502–11
[28] Mo C *et al* 2018 Formation and stability of ultrasonic generated bulk nanobubbles *Chin. Phys. B* **27** 118104
[29] Qiu J *et al* 2017 Formation and stability of bulk nanobubbles generated by ethanol–water exchange *Chem. Phys. Chem.* **18** 1345
[30] Weijs J H, Seddon J and Lohse D 2012 Diffusive shielding stabilizes bulk nanobubble clusters *Chem. Phys. Chem.* **13** 2197
[31] Gao Z *et al* 2021 Understanding the stabilization of a bulk nanobubble: a molecular dynamics analysis *Langmuir* **37** 11281
[32] Hewage S A and Meegoda J N 2022 Molecular dynamics simulation of bulk nanobubbles *Colloid Surf.*A **650** 129565
[33] Dixit A K and Das A K 2022 Molecular approach for understanding the stability, collision, and coalescence of bulk nanobubbles *Langmuir* **38** 16122
[34] Zhang H *et al* 2022 The fate of bulk nanobubbles under gas dissolution *Phys. Chem. Chem. Phys.* **24** 9685
[35] Hoar T and Schulman J 1943 Transparent water-in-oil dispersions: the oleopathic hydro-micelle *Nature* **152** 102
[36] Schulman J, Stoeckenius W and Prince L 1959 Mechanism of formation and structure of microemulsions by electron microscopy *J. Phys. Chem.* **63** 1677
[37] Danielsson I and Lindman B 1981 The definition of microemulsion *Colloids Surf.* **3** 391
[38] De Gennes P G and Taupin C 1982 Microemulsions and the flexibility of oil/water interfaces *J. Phys. Chem.* **86** 2294
[39] Langevin D 1992 Micelles and microemulsions *Annu. Rev. Phys. Chem.* **43** 341
[40] Oberdisse J and Hellweg T 2017 Structure, interfacial film properties, and thermal fluctuations of microemulsions as seen by scattering experiments *Adv. Colloid Interface Sci.* **247** 354
[41] Gradzielski M *et al* 2021 Using microemulsions: formulation based on knowledge of their mesostructure *Chem. Rev.* **121** 5671

[42] Slomkowski S *et al* 2011 Terminology of polymers and polymerization processes in dispersed systems (IUPAC recommendations 2011) *Pure Appl. Chem.* **83** 2229
[43] McClements D J 2012 Nanoemulsions versus microemulsions: terminology, differences, and similarities *Soft Matter* **8** 1719
[44] Winsor P A 1948 Hydrotropy, solubilisation and related emulsification processes *Trans. Faraday Soc.* **44** 376
[45] Winsor P 1954 *Solvent Properties of Amphiphilic Compounds* (London: Butterworths Scientific Publications)
[46] Jin J *et al* 2020 Dynamic tracking of bulk nanobubbles from microbubbles shrinkage to collapse *Colloids Surf.* A **589** 124430
[47] Satpute P and Earthman J 2021 Hydroxyl ion stabilization of bulk nanobubbles resulting from microbubble shrinkage *J. Colloid Interface Sci.* **584** 449
[48] Helfrich W 1973 Properties of lipid bilayers: theory and possible experiments *Z. Naturforsch. C* **28** 693
[49] Peliti L and Leibler S 1985 Effects of thermal fluctuations on systems with small surface tension *Phys. Rev. Lett.* **54** 1690
[50] Szleifer I *et al* 1988 Curvature elasticity of pure and mixed surfactant films *Phys. Rev. Lett.* **60** 1966
[51] Binks B P *et al* 1989 Measurement of film rigidity and interfacial tensions in several ionic surfactant-oil-water microemulsion systems *Langmuir* **5** 415
[52] Gradzielski M, Langevin D and Farago B 1996 Experimental investigation of the structure of nonionic microemulsions and their relation to the bending elasticity of the amphiphilic film *Phys. Rev. E* **53** 3900
[53] Helfrich W 1985 Effect of thermal undulations on the rigidity of fluid membranes and interfaces *J. Phys. France* **46** 1263
[54] Nielsen S O *et al* 2003 Molecular dynamics investigations of lipid Langmuir monolayers using a coarse-grain model *J. Phys. Chem. B* **107** 13911
[55] Ybert C *et al* 2003 Collapse of a monolayer by three mechanisms *J. Phys. Chem. B* **106** 2004
[56] Lee K Y C 2008 Collapse mechanisms of Langmuir monolayers *Annu. Rev. Phys. Chem.* **59** 771
[57] Marmottant P *et al* 2005 A model for large amplitude oscillations of coated bubbles accounting for buckling and rupture *J. Acoust. Soc. Am.* **118** 3499
[58] Baoukina S 2008 The molecular mechanism of lipid monolayer collapse *Proc. Natl Acad. Sci. USA* **105** 10803
[59] Schlesinger I and Sivan U 2018 Three-dimensional characterization of layers of condensed gas molecules forming universally on hydrophobic surfaces *J. Am. Chem. Soc.* **140** 10473
[60] Li Z *et al* 2013 Effect of airborne contaminants on the wettability of supported graphene and graphite *Nat. Mater.* **12** 925
[61] Kozbial A *et al* 2014 Understanding the intrinsic water wettability of graphite *Carbon* **74** 218
[62] Nioradze N *et al* 2015 Organic contamination of highly oriented pyrolytic graphite as studied by scanning electrochemical microscopy *Anal. Chem.* **87** 4836
[63] Ducker W A 2009 Contact angle and stability of interfacial nanobubbles *Langmuir* **25** 8907
[64] Das S, Snoeijer J H and Lohse D 2010 Effect of impurities in description of surface nanobubbles *Phys. Rev. E* **82** 056310
[65] Lohse D and Zhang X 2015 Surface nanobubbles and nanodroplets *Rev. Mod. Phys.* **87** 981
[66] Maheshwari S *et al* 2016 Stability of surface nanobubbles: a molecular dynamics study *Langmuir* **32** 11116